ASE-1825

FINAL REPORT

A CONTINUATION OF A PROGRAM OF HIGH ANGULAR RESOLUTION STUDIES OF CELESTIAL X-RAY SOURCES

CONTRACT NASW-1634

REPORT PERIOD 6 JULY-29 DECEMBER 1967

PREPARED FOR

NATIONAL AERONAUTICS AND SPACE ADMINISTRATION

4 JANUARY 1968

AMERICAN SCIENCE AND ENGINEERING

11 Carleton Street, Cambridge, Massachusetts 02142

AS&E

ASE-1825

FINAL REPORT

A CONTINUATION OF A PROGRAM OF HIGH ANGULAR RESOLUTION STUDIES OF CELESTIAL X-RAY SOURCES

Contract NASW-1634

REPORT PERIOD

6 July 1967 to 29 December 1967

Prepared for

National Aeronautics and Space Administration

NASA Headquarters

Washington, D. C. 20546

Prepared by

American Science and Engineering

11 Carleton Street

Cambridge, Massachusetts 02142

Date: 4 January 1968

FOREWORD

This document is the final report on NASA Contract NASW-1634. This contract is part of a continuing program of X-ray astronomy by AS&E and calls for the refurbishment of an instrumented payload plus the addition of a new background discrimination system. The payload has been flown from an Aerobee rocket and some of the instrumentation readings have been analyzed. The experimental objectives were not attained due to a failure of the door control mechanism. The payload has been recovered intact and will be flown again in the near future. The authors of this report are H. Gursky, R. Giacconi, P. Gorenstein and H. Manko.

ACKNOWLEDGMENTS

We wish to acknowledge the contributions of the following individuals at AS&E to this program. Mr. A. DeCaprio, the Project Mechanical Engineer, and Mr. S. Mickiewicz were responsible for the design, fabrication and testing of the payloads in their respective areas. Additional engineering support was obtained from Mr. W. Antrim, Director of the Mechanical Department, Mr. A. B. Johnson, Director of Engineering, and Mr. G. Sinnamon, Director of the Systems Department.

We also wish to acknowledge many fruitful discussions with Dr. Martin Annis, Dr. Jack Carpenter, and Dr. Oscar Manley of AS&E and Professor Bruno Rossi of MIT.

TABLE OF CONTENTS

LIST OF TABLES

1. INTRODUCTION

The objectives of this experimental program followed from the results we had obtained from the preceding rocket flight. The principal observations were as follows:

1. An identification of the X-ray source Cyg X-2 with a bluish, variable, visible object.

2. The absence of X-ray emission from Cygnus A, the extra-galactic radio source, at a level of intensity observable from rockets.

3. A distribution of X-ray sources that strongly suggested that they are associated with the spiral arm structure of the galaxy.

4. The existence of a deficiency in the number of photons in the low energy part of the spectrum for several of the X-ray sources.

The conclusion derived from observation (3) suggests a particular distribution for X-ray sources along that portion of the galactic equator which lies between $\ell^{II} = 100^{\circ}$ and $\ell^{II} = 260^{\circ}$. In particular, sources are expected in the Cepheus-Lacertus region because of the presence of the Perseus spiral arm and in the Orion region because of the Orion arm. Although this part of the galactic equator has not been observed with the same sensitivity as the part between $\ell^{II} = -15^{\circ}$ and $\ell^{II} = 100^{\circ}$, the NRL group has reported several sources in the former region. In addition, if observation (4) results from interstellar attenuation, then a correlation is expected between the low energy deficiency and the integrated mass density to the source which is related to its distance along a certain direction. Hence a measurement of the distribution and spectra of X-ray sources between 100° and 260° would test various hypotheses of the spiral arm model:

1. The presence of sources in certain regions along the galactic equator and not others.

2. General correlation of intensity at the earth with location based on distance to the relevant spiral arm and the assumption that groups of X-ray sources have the same average inherent intensity.

3. General correlation of low energy photon deficiency with location based on distance to spiral arm, and the assumption that interstellar attenuation is the reason for the deficiency.

Other objectives of this experiment include the following:

1. Determination of X-ray source locations precise enough (10 arc min x 10 arc min) to allow the possibility of making identifications with specific visible or radio objects. Of particular interest are the radio sources Cas A and SN 1572 which are believed to be remnants of supernova explosions.

2. A measurement of the spectrum of the Crab Nebula. The presence of a low energy deficiency would almost definitely be a result of interstellar attenuation because its large spatial extent (~ 1 pc) precludes self-absorption. Since the distance to that object is known (1300-1700 pc), the spectral measurement would determine the density of middle Z elements in the interstellar medium.

3. A measurement of the X-ray background along the galactic equator from $\ell^{II} = 100^{\circ}$ to $\ell^{II} = 260^{\circ}$ and perpendicular to the equator at $\ell^{II} = 115^{\circ}$ to look for any anisotropies.

2. EXPERIMENT PLAN

The X-ray detectors were to observe out the side of the payload (along - yaw axis) behind two slat collimators. Each collimator had a field of view of 2° by 40° full width at half maximum. The two 2° fields of view were offset from the plane normal to the roll axis by $+30^{\circ}$ and -30°. Hence the location of an X-ray along two lines intersecting at a 60° angle could be attained in a single scan. The precise location (several arc minutes) of the X-ray field of view upon the celestial sphere was to be obtained by photographing the star field with an aspect camera located between the two collimators.

A standard ACS system controlled the aspect of the vehicle. The experimental program consisted of maneuvering the vehicle successively through a sequence of several targets. However, no time was spent actually pointing at the targets. The observation periods were the controlled rate of scan between pointing positions. In this manner certain regions along the galactic equator were scanned at a rate of 2°/sec, another at 1°/sec and parts of the Cassiopeia, Cepheus, and Lacertus constellations at $3/4^{\circ}$/sec in a series of maneuvers that included several scans at various angles to the equator. At the fastest rate of scan, 2°/sec, the minimum detectable source (each collimator) was to have been 0.035 counts/sec (2-5 keV) which is about 2×10^{-3} Sco X-1. At the slower rate of scan the location determination capability was about 10-20 arc minutes.

3. HARDWARE DESIGN

The payload for NASA Aerobee Rocket 4.228 CG came from a refurbishment of the payload of 4.149 CG. The major changes that were made included a more intricate mechanism for opening and closing the door, the replacement of two of the eight active proportional counters by proportional counters having thinner windows, and a new electronic system to reduce cosmic background. A description of the system is given in the appendix.

3.1 Aspect Camera

The camera which had been flown twice previously, and performed to expectations, was a 16 mm Millikan Model DBM-3C, with an Angenieux f/.95, 25 mm focal length lens. Figure 1 is a picture of the camera and associated hardware.

3.2 Proportional Counters

Three types of proportional counters were used on this flight. Of the twenty counters flown, six had 2 mil beryllium windows, two had 1 mil beryllium windows, and 12 had thick aluminum windows. The beryllium window (active) counters were filled with P10 (90% Argon and 10% Methane) and had overall dimensions 16" x 2" x 2" with an effective window area of 14.81 x 1.75" minus a considerable loss due to the presence of a support structure. The thick window (guard) counters were filled with Xenon and had overall dimensions of 16" x 2" x 1". The counters were set up in two banks with 4 active counters in front, enclosed by 6 guard counters on 3 sides in each bank. Figure 2 shows the layout of an active counter bank with a guard counter on each side. Figure 2 also shows the layout of the remaining guard counters which are mounted directly behind the active counters. Location of the preamp for each proportional counter can also be seen.

Any cosmic ray event which was able to penetrate the active counters and reach the guard counters would produce a veto signal which would block out the corresponding signals generated in the active counters. A

ASPECT CAMERA ASSEMBLY

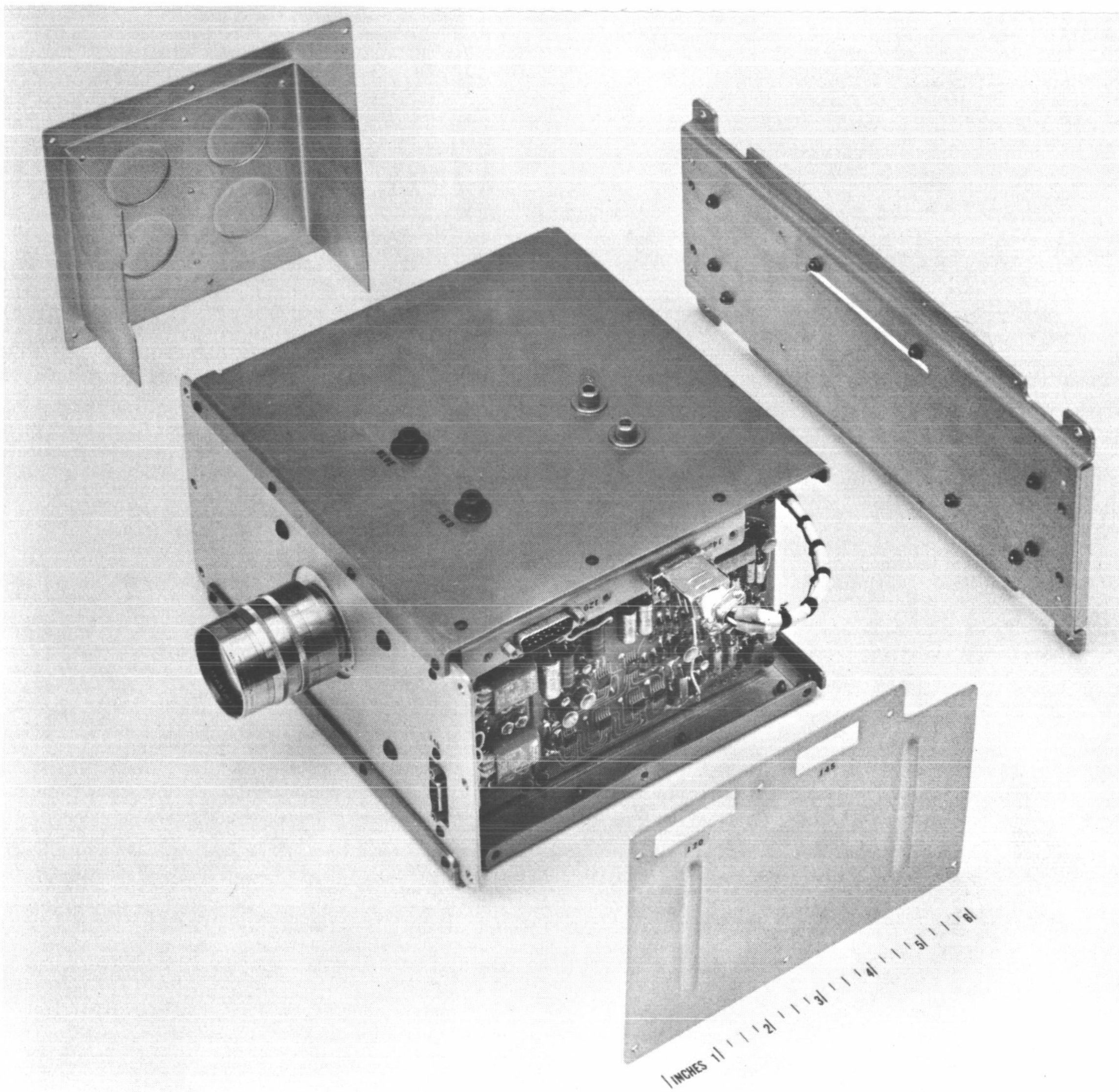

DO-006

Figure 1

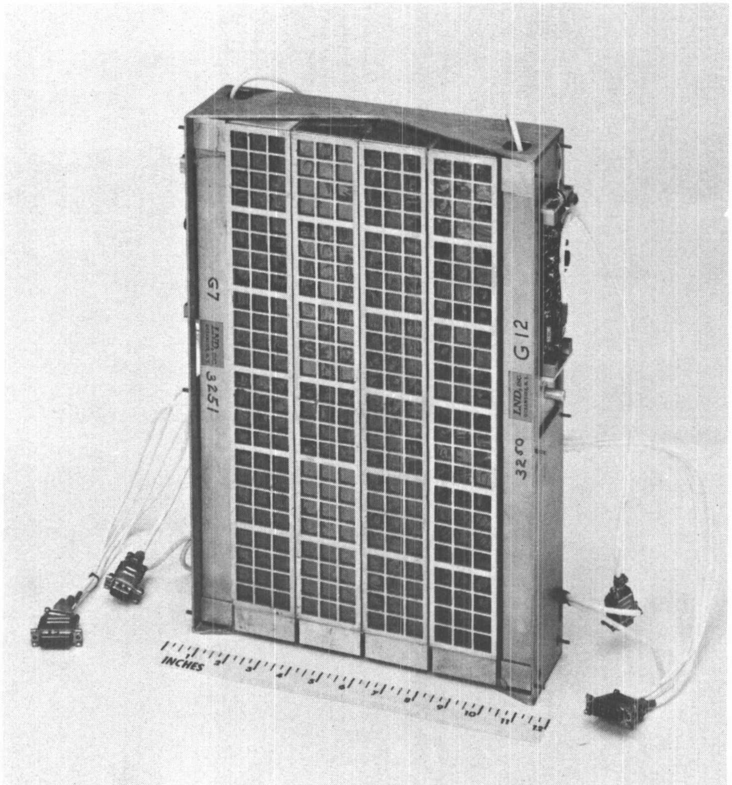

DO-017

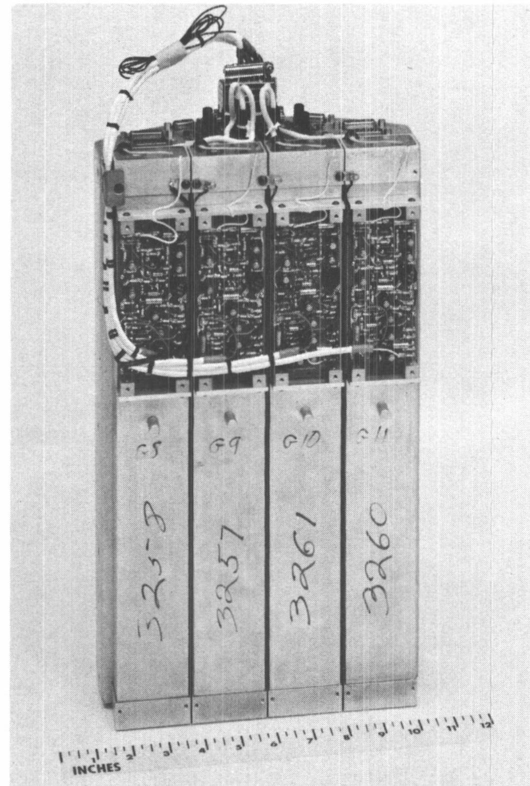

DO-018

PROPORTIONAL COUNTER ASSEMBLIES

Figure 2

$3\mu s$ delay line was added to the logic circuitry to compensate for any delays which might occur in the development of the veto signal in the guard counters. Figure 3 is a block diagram of the proportional counter logic used. Digital information was supplied by each active counter, and two active counters were combined for the pulse height information. Two scalers, one pulse height analog channel and two log count rate meter outputs were supplied by each of four separate logic circuits. Figure 4 is a block diagram of the preamp circuit used for each of the counters.

3.3 Collimators

Two slat-type collimators, one in front of each bank of counters, were used to limit the acceptance directions of the X-rays to a field of view of $2^{o} \times 40^{o}$ (full width half maximum). The two sets of slats were inclined $+30^{o}$ and -30^{o} from a plane normal to the roll axis of the rocket. The overall dimension of each collimator bank was 15" x 8 1/2" x 5 1/2". The individual slats were made of iron and spaced a distance of .160". The collimators and their relation to the camera are seen in the fully assembled payload shown in Figure 5. A close-up view of the collimators is shown in Figure 6.

3.4 Telemetry

The telemetry used in this payload consisted of two Model SST-3, PPM/AM systems operating at a 20 KCPS sampling rate and were developed and supplied by NASA-GSFC. The operating frequencies for the two transmitters were 234.0 MHz and 244.3 MHz, with the experiment section using 12 of the 15 channels available on each transmitter. Table I contains a list of the channels and the information transmitted on each channel. Four of the signals on each transmitter required increased frequency response, and therefore two channels were used on each of them.

Table II gives the function transmitted on each of the channels that carried the commutator data from the experiment.

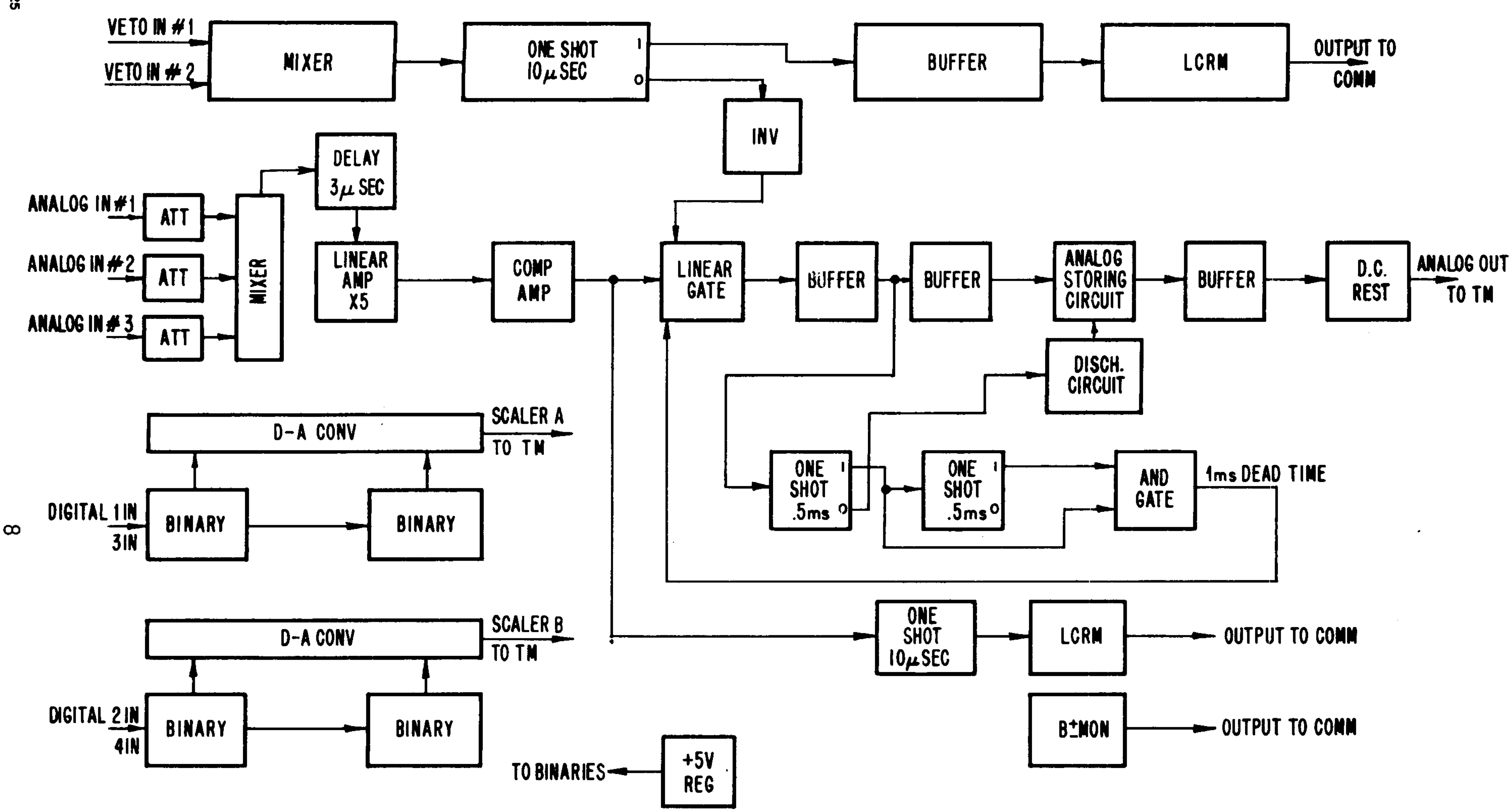

PROPORTIONAL COUNTER LOGIC

1825

Figure 3

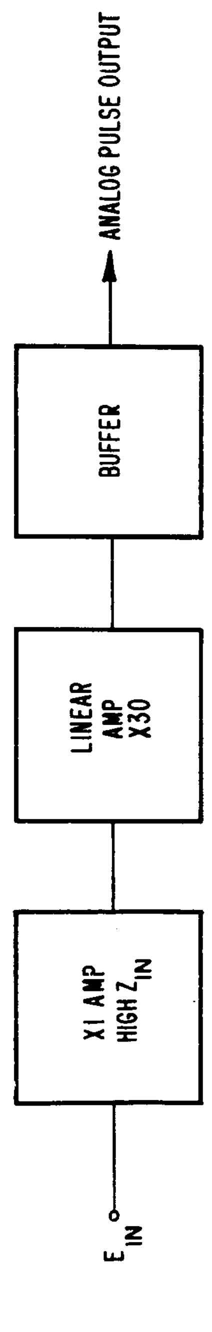

PROPORTIONAL COUNTER PREAMP

VIEWS OF ASSEMBLED PAYLOAD

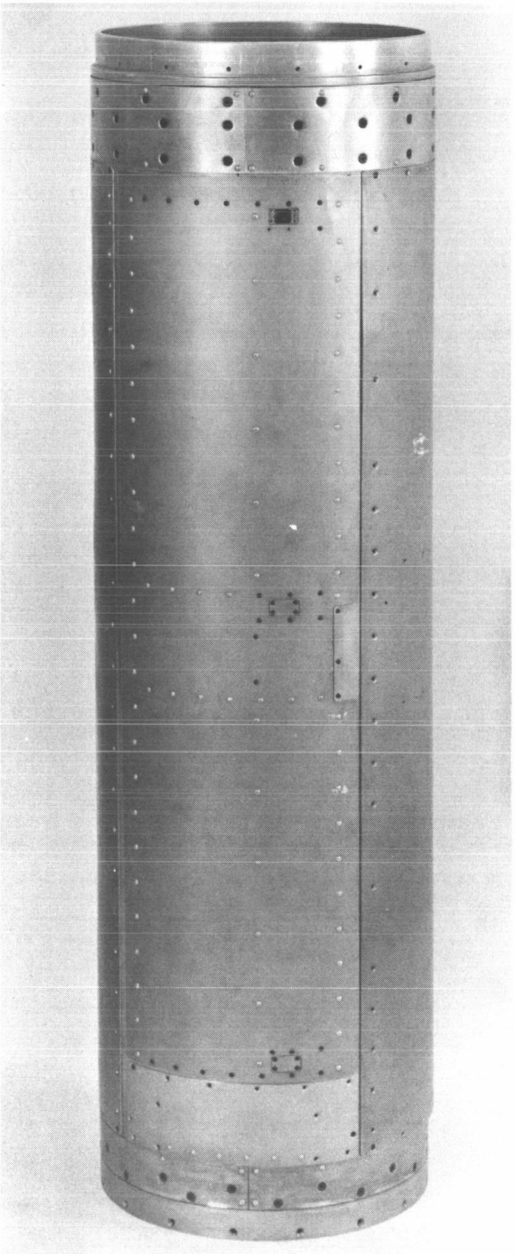

DY-001

CLOSED

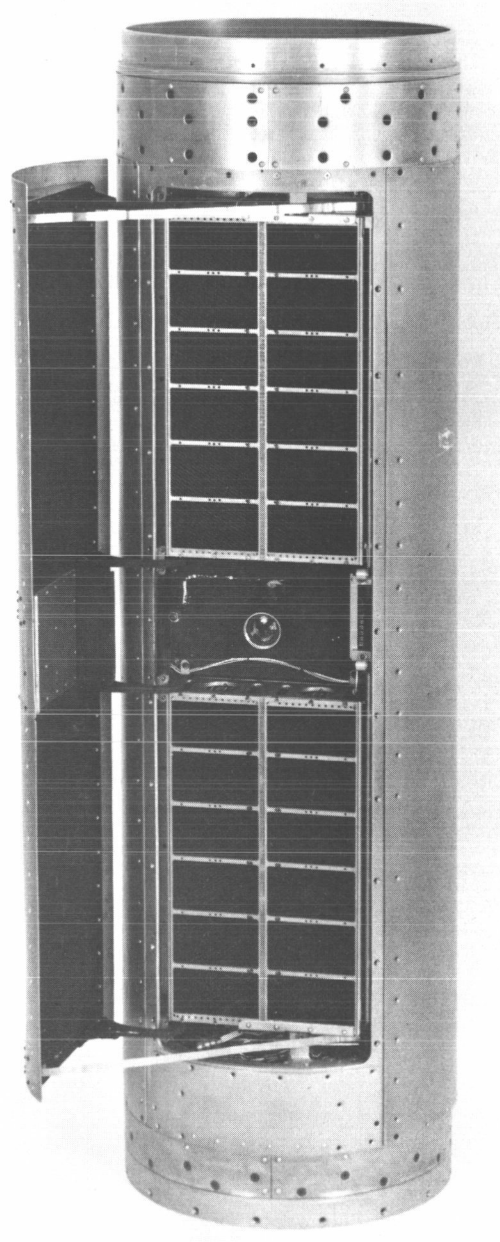

DY-002

OPEN

Figure 5

CLOSE-UP OF COLLIMATOR IN ASSEMBLED PAYLOAD

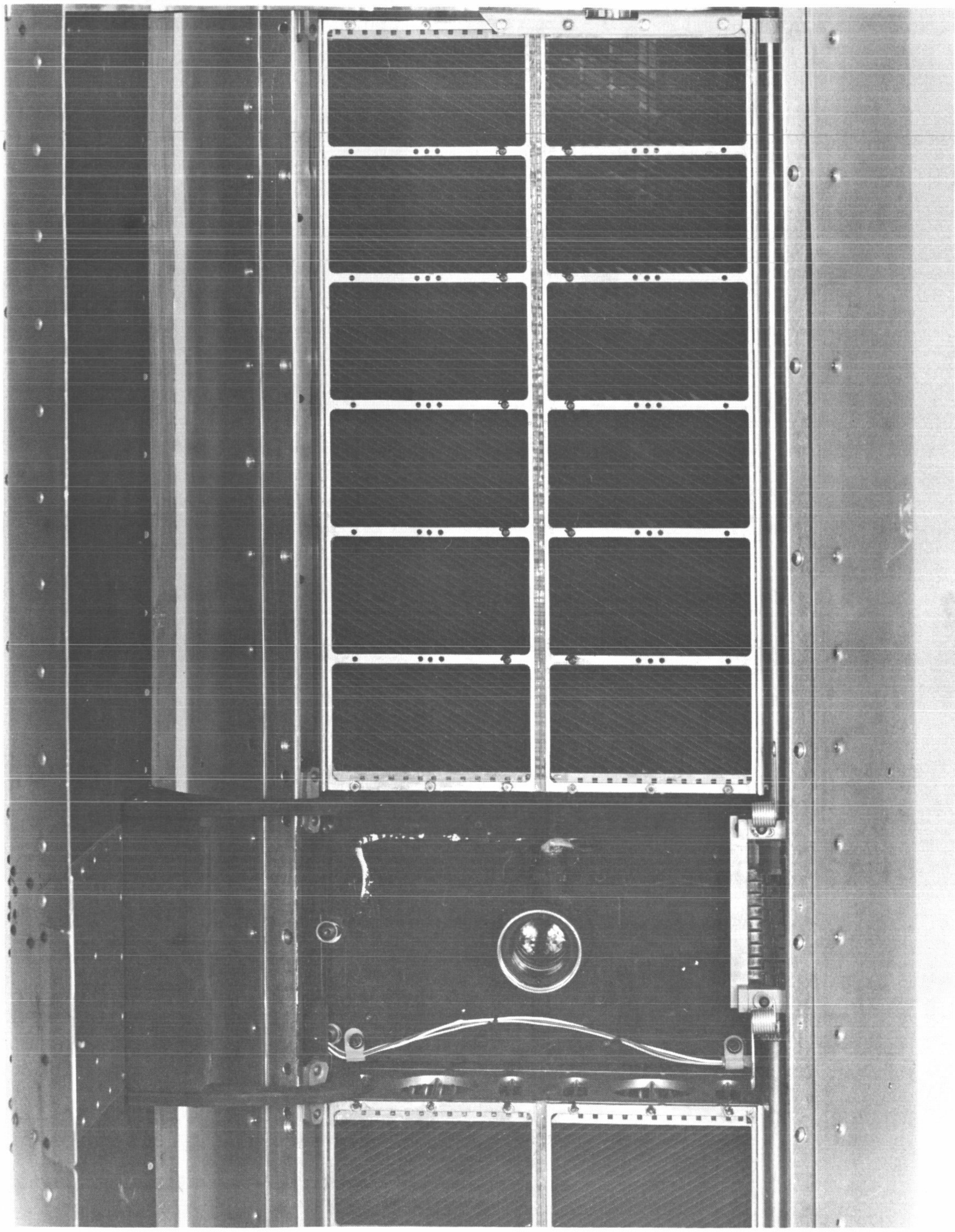

DY-003

Figure 6

3.5 ACS

The maneuvers scheduled by the ACS system are listed in Table III, along with the time-in position and the T+ time the maneuver occurred.

The first nine maneuvers are involved in correcting for the actual launch attitude in order to line up the rocket axes at the desired starting point.

At the beginning of position 10, the vehicle was programmed to be oriented with its -yaw axis (nominally the axis of the X-ray detectors) at the position R. A. = $8^{hr}\ 54^{m}\ 12^{s}$, $\Delta = -45^{\circ}\ 04'$ which is on the galactic equator at an $\ell^{II} = 265^{\circ}$. The -pitch axis was aligned to the galactic pole; thus maneuvers 1 and 2 (Ledex positions 10 & 11) carried the -yaw axis along the galactic equator towards lower longitude.

TABLE I

TELEMETRY CHANNEL ALLOCATIONS

Telemetry System #1 (234.0 MHz)

Data	Channel
Pha (c)	2 and 10
Psd (a)	3 and 11
Psd (c)	4 and 12
Pha (a)	5 and 13
Scaler (d)	6
Scaler (b)	7
Commutated (exp.)	8
Roll and despin valves	9
Pitch valves	14
Accel./roll position	15
Fiducial light	16

Telemetry System #2 (244.3 MHz)

Data	Channel
Pha (b)	2 and 10
Psd (d)	3 and 11
Pha (d)	4 and 12
Psd (b)	5 and 13
Scaler (c)	6
Ledex and yaw valves	7
Commutated (exp.)	8
Clock	9
Commutated (instr.)	14
Pc/Yaw position	15
Scaler (a)	16

TABLE II

COMMUTATED CHANNEL

Transmitter #1 (234.0 MHz)

Segment	Data
1 - 9	Synchronization Pulses
10	Spare
11	7.5 V Internal Power Monitor
12	Door Open Monitor
13	Spare
14	Spare
15	Spare
16	Not used
17	Not used
18	Not used
19	Spare
20	Spare
21	P.C. LCRM-A
22	P.C. LCRM-C
23	P.C. HV Monitor B
24	P.C. HV Monitor D
25	Guard No. 1 HV Monitor
26	Guard LCRM-A
27	Guard LCRM-C
28	P.C. Cutoff Mon. No. 1
29	P.C. Cutoff Mon. No. 3
30	P.C. Cutoff Mon. No. 5
31	P.C. Cutoff Mon. No. 7
32	Spare
33	Spare
34	B+ Mon. A
35	B+ Mon. C
36	+6.75 V Monitor No. 1
37	Door Batt. No. 1 Mon.
38	+9 V Monitor
39	Timer No. 1 Operate Mon.
40	28 V Monitor No. 1
41	28 V Camera Batt. Mon.
42	+6.75 V Reg. No. 1 Monitor
43	5.0 V Calibrate
44	2.5 V Calibrate
45	0 V Calibrate

TABLE II - cont'd

COMMUTATED CHANNEL

Transmitter #2 (244.3 MHz)

Segment	Data
1 - 9	Synchronization Pulses
10	Spare
11	7.5 V Internal Power Monitor
12	Door Closed Monitor
13	Spare
14	Spare
15	Spare
16	Not used
17	Not used
18	Not used
19	Spare
20	Spare
21	P.C. LCRM-B
22	P.C. LCRM-D
23	P.C. HV Monitor A
24	P.C. HV Monitor C
25	Guard No. 2 HV Monitor
26	Guard LCRM-B
27	Guard LCRM-D
28	P.C. Cutoff Monitor #2
29	P.C. Cutoff Monitor #4
30	P.C. Cutoff Monitor #6
31	P.C. Cutoff Monitor #8
32	Spare
33	Camera Monitor
34	B+ Monitor B
35	B+ Monitor D
36	6.75 V Monitor #2
37	Door Batt. #2 Monitor
38	Not Used (2V)
39	Timer #2 Operate Monitor
40	28 V Monitor #2
41	28 V Instr. Batt. Mon.
42	+6.75 V Reg. #2 Monitor
43	5.0 V Calibrate
44	2.5 V Calibrate
45	0 V Calibrate

TABLE III

4.228 ACS PROGRAM

Function	Maneuver, Rate	Rotation Angle	Time of Man.	Total Elapsed Time
Start				53
Coast			11.1	64.1
Despin			12	76.1
Erect			12	88.1
Coast			2	90.1
Roll Remote Adj.			3	93.1
Pitch Remote Adj.			3	96.1
Yaw Remote Adj.			3	99.1
Coast			2.6	101.7
Roll	5°/sec	12°	2.4	104.1
Pitch	-2°/sec	-76°	38	142.1
Pitch	-1°/sec	-10°	10	152.1
Pitch	-2°/sec	-40°	20	172.1
Pitch	-0.75°/sec	-40°	54	226.1
Yaw	-5°/sec	-30°	6	232.1
Pitch	$+0.75^{\circ}$/sec	26°	35	267.1
Yaw	-5°/sec	-30°	6	273.1
Pitch	-0.75°/sec	-36°	48	321.1

4. TESTING AND CALIBRATION

4.1 Testing

Work was initiated on the payload early in June, at which time the pre-shoot conference was held at NASA-GSFC. Rework and fabrication of new parts was completed by the end of September 1967, and a completely assembled payload was available by 8 October 1967, ready for testing. The following schedule was adhered to until launch:

12 October 1967	Completion of all System Testing
13 October 1967	Vibration Testing
18 October 1967	Start Integration at GSFC
23 October 1967	Vacuum Testing
24 October 1967	Start Instrument Alignment at AS&E
6 November 1967	Personnel and Equipment arrive at WSMR, N. M.
20 November 1967	Launch

A preliminary test of a sample electronics unit and an SST-3 telemetry system was conducted at GSFC on 20 July 1967 to verify that our electronics is compatible with the SST-3 which had not been used by AS&E prior to this time.

System Tests

A standard system test was performed on the payload to verify proper operation of (a) all instruments, (b) power and control system, (c) door operate mechanism, (d) TM data readout at the TM interface including commutated data, and (e) compatibility and operation of the ground control console. Satisfactory completion of this test was a prerequisite for any further testing.

Vibration Test

The payload was subjected to a random noise vibration test at the following levels:

Payload Axis	Freq. Range	Level	Duration	PsD Level
Thrust	20-2000 cps	10g rms	60 sec.	$.05g^2/cps$
2-Lateral	20-2000 cps	6.2g rms	60 sec.	$.025g^2/cps$

The payload was not operated during the vibration tests; however, a complete functional test was performed immediately after the vibration test. Visual inspection and all electrical tests showed no damage or erratic operation because of the shaking.

Integration Tests

Payload/TM/ACS integration tests were conducted at GSFC on 18 and 19 October 1967. Some RFI was observed during testing due to the type and location of transmitting antennas used for the integration tests. The location of the antennas was not as in the flight configuration. The only other minor problem was the door reset command which occurred at about 52 seconds instead of 62 seconds. This was corrected by the ACS people.

Vacuum Test

The payload was operated in a vacuum chamber to a pressure of 2×10^{-4} mmHg. All instruments worked properly and the door was operated. The door opened normally but would not close on command. A visual inspection showed that the door motor shutoff microswitch was stuck, completely depressed, thus preventing the door motor from operating. The switch was replaced and the door continued to open and close satisfactorily.

Static Load Test

Since this payload has had two static load tests performed for its previous flights (4.148 and 4.149 CG) no further static load test was performed for this flight.

4.2 Calibration and Alignment

Calibration of the X-ray proportional counters was carried out by exposing each detector to a series of radioactive X-ray sources ranging in photon energy from 1.5 to 22 keV. In this manner the overall response of the counters and amplifiers were measured, the desired gain and bias were established, and the energy resolution of the system was determined over that range of energy. In addition, a Co^{60} source was used to simulate cosmic background in the calibration of the rise time discrimination system.

The rigidity of the payload was such that the alignment of the aspect camera and the X-ray collimators would be maintained throughout the launch and duration of the flight. However, it was essential to measure their relative alignment in the laboratory prior to flight. Through knowledge of the alignment, the location of an X-ray source could be determined from the observance of a counting rate peak at a certain time and the aspect photographs. This was achieved by setting up an "X-ray" star in the laboratory. Several light beams and an X-ray beam were made parallel to each other by collimating each through the same two rigid plates. The entire payload was set upon a rotary table with both the aspect camera and X-ray detectors in operation, as shown in Figure 7. The payload is positioned such that the camera views one of the light beams. As the rotary table is turned, a maximum is observed in the counting rate. At exactly that point a photograph is taken. Inspection of the photograph reveals where on the photograph the X-ray star will appear. The camera registration was sufficiently precise, such that the sprocket holes of the film could be used as a reference. This technique enabled us to establish the alignment to within several arc minutes.

Collimator plate #1 consisted of a series of holes (1/4" dia for X-ray, 1/16" dia for visible light), spaced 3" apart. Collimator plate #2 was a series of slits 1" high whose spacing matched that of plate #1. It contained a 4" opening for the X-rays and several 1/16" openings for the light.

The X-ray and light sources were removed 80' from the payload. Consequently, the X-ray beam was collimated to 17 arc min. by the 4" opening and the light beams were collimated to less than 1/2 arc min. Several passes were needed to sample the entire 32" of collimator length. As the low energy X-ray flux would be utterly attenuated by 80' of air, a beam tube containing 1 atmosphere of helium was used between the plates as the means of transmitting the X-rays.

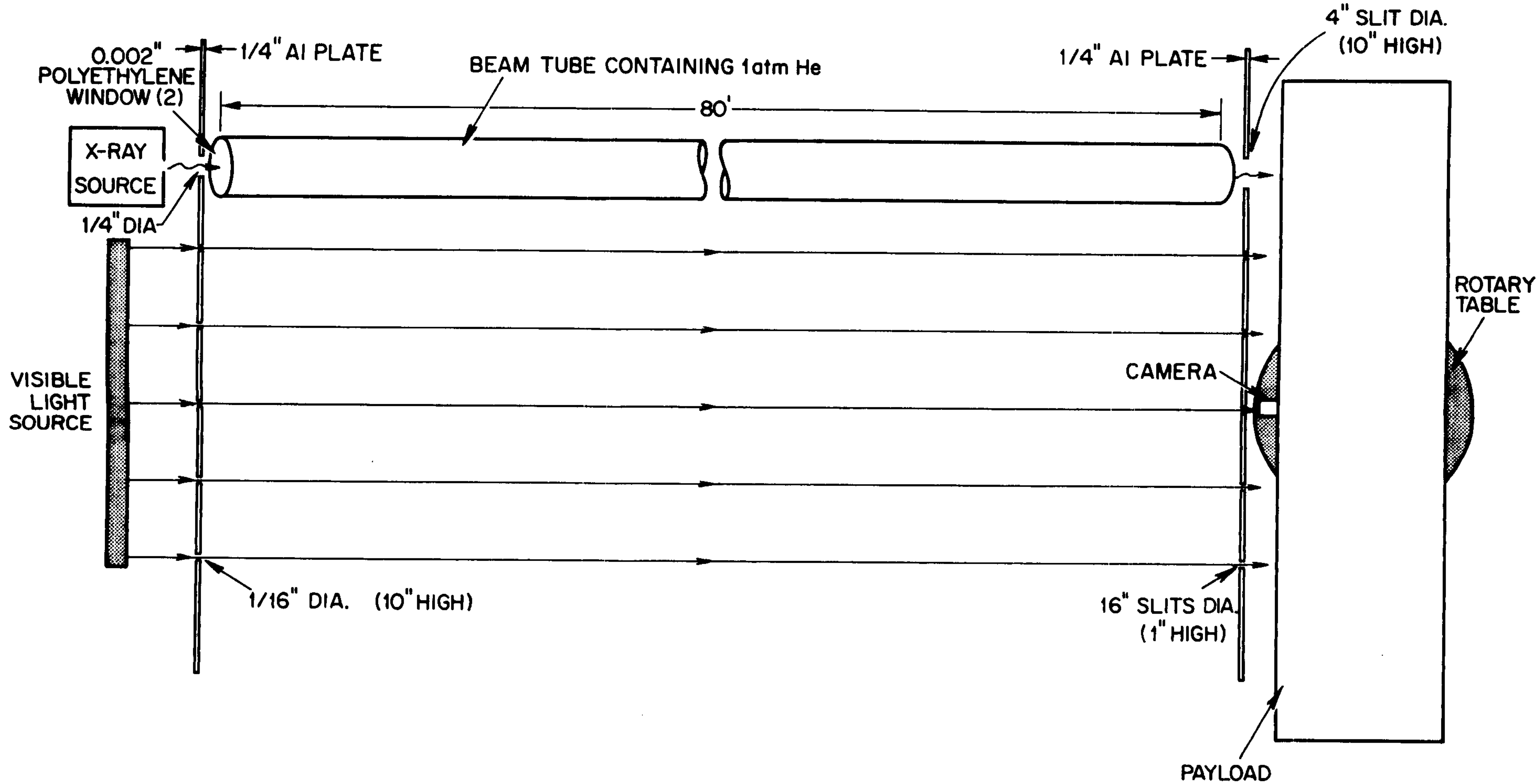

MEASUREMENT OF CAMERA-COLLIMATOR ALIGNMENT

Figure 7

5. FLIGHT 4.228 CG

On 6 November 1967 the payload and personnel arrived at WSMR. A schedule of events to launch follows:

8 November 1967	Pre-flight Conference
15 November 1967	Horizontal Check
16 November 1967	Rocket Installed in Tower B
17 November 1967	Vertical Check
20 November 1967	Launch

During the first week, two of the two mil window proportional counters were replaced with counters with one mil windows. The calibration of the instruments was checked daily, and additional star pictures were taken with the payload camera during the preparation time to verify its operation. In addition, star pictures were taken in the testing of two different types of high-speed film to determine which film had optimum sensitivity. At 0342 MST on 20 November 1967 the payload was launched.

The vehicle did reach the anticipated peak altitude; however, the residual sustainer pressure used to operate the ACS system was considerably below normal.

The door on the experimental portion of the payload did not open at the specified time nor at any time during the flight in which useful data could be obtained.

Several factors that have a bearing or could have a bearing on the failure of the door system are listed below.

1. From the paper oscillographic records it was found that at 42 seconds the door close monitor, a micro-switch, was able to move and showed the door no longer fully closed. At 79 seconds no door open indication was observed from the door open monitor. Both indications above did not change for the remainder of the flight till severance. After severance no data is transmitted.

2. The door release guillotines were expended and the bolts cut as observed from the recovered payload. The door cables which close the door were also observed to be properly wound. To be properly wound the cables must have been unwound and then rewound in the opposite direction. This indicates

that at some time during the flight the door must have opened completely.

3. The developed flight film showed that during the flight there were only two frames exposed to light. These frames were found to be at =T + 326 seconds which is sustainer severance. The observations in sections 2 and 3 now indicate that apparently due to the shock of severance on the payload, the door opened and was immediately closed again. The time between the door opening and closing is about 3 1/2 seconds and thus accounts for the two exposed pictures.

4. Further visual observations of the payload showed the following mechanical and physical damage:

    a. The lower half of the door was found to be sprung open about 1/4".

    b. The rivets holding the door reinforcing rib to the door panel were sprung on the lower half of the right side of the door (opposite side of hinges). Two rivets on the lower left side of the door were also loose.

    c. The bottom edge of the door panel was curled out, and a section of the panel between the loose rivets and a second row of rivets holding the rib had been pushed in flat from the normal door radius.

    d. All three panels, except the door, showed signs of heating, enough to discolor the irriditing on both sides of the panels. These panels also had dents in them but showed no scratches at these points.

5. A test was run with the door and adjacent panel to see if heating of the panel would cause sufficient buckling to keep the door from being opened. A propane torch was applied to the edge of the panel nearest the hinges, and the door was released. The door opened a fraction and then jammed between the door edge and edge of the panel. This occurred

for a few seconds, and apparently after the panel cooled sufficiently the door opened completely.

6. The timing functions were checked and were found to be as previously set. A checkout of the payload also proved everything is working satisfactorily.

7. The nose cone and tip were not damaged in any way except for discoloration of the coating on the 6" nose tip.

8. The payload was found in a level sandy clearing on recovery. It was lying on the door panel. There were no signs of the payload being dragged.

Conclusions indicate that either at lift-off or during powered flight around 42 seconds aerodynamic buffeting and/or heating caused the door to jam and was not freed till the shock of severance.

A possibility also exists that the indication in item 1 occurred due to internal pressure of the payload. This would indicate that additional venting would be required in addition to normal seams and leakage paths.

It appears that all electronics systems did operate successfully during the flight. This will provide, at least, useful information on the efficacy of the background discrimination system.

The payload was recovered on 22 November 1967. Little structural damage was sustained and all electronic systems were operating when the payload was returned to AS&E.

6. DATA

The failure of the door to open until very late in the flight means that no useful cosmic X-ray data will be obtained.

However, the flight appears to have established the ability of the rise time discrimination system to reduce the cosmic background considerably. As expected, a large number of events were recorded through the closed door even though the anticoincidence counters were operating well. Throughout the entire energy range, about 100 counts/sec over 200 cm^2 effective area were observed. Of these 25% fell in the energy range 3-10 keV. An analysis of the rise time spectrum of the 3-10 keV cosmic events shows it to be quite similar to the broad spectrum of events caused by a Co^{60} source. Hence it is expected that the rise time discrimination method used to distinguish X-ray and Co^{60} events in the ground calibrations will be just as effective in flight for suppressing cosmic background events. The system is described in the appendix.

APPENDIX A

REDUCTION OF COSMIC BACKGROUND IN AN X-RAY PROPORTIONAL COUNTER THROUGH RISE TIME DISCRIMINATION

Paul Gorenstein and Stanley Mickiewicz

American Science and Engineering
Cambridge, Massachusetts

INTRODUCTION

Since the discovery of cosmic X-ray sources by Giacconi, Gursky, Paolini and Rossi[1] great efforts have been made to extend the sensitivity of the space borne detectors used in the X-ray astronomy observations. Proportional counters have been used extensively because of the ability to fabricate these devices with large area and comparatively large efficiency in the 1-50 keV region, plus the necessity of obtaining spectral information from the discrete X-ray sources. A basic limitation upon the sensitivity of such detectors in observations requiring good spatial resolution has been the presence of a non-X-ray background induced by cosmic rays. The system described here utilizes the principle of Mathieson and Sanford[2] to reduce this background. It has the potential for enormously increasing the sensitivity of high resolution X-ray surveys.

Anticoincidence guard counters behind the X-ray detectors succeed in removing only a part of the non-X-ray background that has been observed in X-ray astronomy experiments. For example, a recent evaluation of the background situation that prevailed during a sounding rocket observation that took place on 11 October 1966[3] indicates that the anticoincidence counters removed only about one-third of the non-X-ray background in the energy range 2-5 keV. (Most probable energy deposit for a minimum ionizing particle was 8 keV.) The residual events are believed to be due to gamma ray interactions occurring in the walls of the detector that eject an energetic electron into the gas volume. The origin of the gamma photon is the interaction of a cosmic ray primary with the payload material or the atmosphere below. Ultimately, a single high energy primary interaction will yield several gamma photons. The guard counters are largely ineffective against this source of background.

Mathieson and Sanford[2] have shown that an X-ray interaction and a gamma induced event of equal energy deposition can be distinguished on the basis of the difference in rise time of the proportional counter signal. Starting from this, we have developed a system applicable to a large area proportional counter of the usual shape. It has the virtue of being simple, compact and readily incorporated into an X-ray astronomy payload. Laboratory measurements on a conventional proportional counter (5 cm x 5 cm x 35 cm) filled with a 1 atm mixture of 90% argon and 10% methane have shown that the system has the capability of rejecting over 90% of the gamma events in the energy range 3-10 keV while at least 75% of the X-ray efficiency is retained. A space qualified version of the system has been built and incorporated into the electronics of an X-ray astronomy sounding rocket payload that shall be flown shortly. It does not require any critical components. With minor modifications it has the capability of good background rejection and high X-ray acceptance over a much larger range of photon energies and possibly even better performance than what has been observed thus far.

DESCRIPTION OF THE RISE TIME DISCRIMINATION SYSTEM

The basis for the discrimination originates in the difference in path length between a photoelectron and an energetic particle depositing the same amount of energy in the counter. Ultimately this results in a difference in rise time between the corresponding output signals. Figure 1 illustrates the principle of operation. The idealized waveforms are shown for two signals of different rise time at three consecutive stages in the system: pre-amp output, after delay line clipping and RC differentiation, and the output of a tunnel diode "zero crossing" discriminator. The output of the zero crossing discriminator is a waveform of almost constant amplitude which begins when the input exceeds a pre-set triggering level and terminates when the input passes through zero. The result is a pulse whose width is nearly proportional to the rise time of the pre-amp signal. By means of a ramp generator the rise time information is converted from a width to an amplitude. It turns out that nearly all X-ray events are characterized by a short rise time, whereas the energetic particle events have a variety of rise times which are for the most part much longer. Hence the X-ray events past the zero crossing discriminator have a very narrow range of amplitudes compared to the background.

A simplified block diagram of the circuits used in the rocket experiment is shown in Figure 2. The essentials of the pre-amplifier consist of a charge sensitive input section (T_1, T_2, T_3, T_4) similar to the one described by Splichal[4]. The pair of transistors T_5 and T_6 are a high gain video amplifier. Additional pre-amp components relating to the telemetry transmission requirements of the rocket are not shown. The finite bandwidth of the pre-amps limited the rise time of the X-ray signals to a minimum of 70 nsec and differentiated the output with a time constant of 2.5 μsec. Two output signals emerged from the pre-amp. One was subsequently used for pulse height analysis while the other was routed to a mixer that received inputs from 4 independent detectors before arriving at the rise time discrimination system. Some slight differences in rise time from the various pre-amps were equalized by an integration before the mixer inputs.

The output of the mixer was clipped by a 100 ohm, 60 nsec shorted lumped constant delay line. A mild RC differentiation was performed upon the resultant waveform to insure its going through zero voltage. After amplification the signal was applied to the zero crossing detector shown in Figure 4 which was adapted from a circuit described by Alston and Draper[5]. This component is, strictly speaking, only a zero crossing detector. Hence the start of the output waveform will depend somewhat upon the amplitude of the input. Small signals will result in a late start and consequently an output of shorter duration. This problem of amplitude dependence could be relieved through the use of a separate time pick-off circuit or an amplifier with larger gain. However, performance under this condition was adequate for the energy range of the intended experiment. It should be pointed out that signals of very long rise time are considerably reduced in amplitude by the delay line clipping. Without large amplification they may no longer be capable of triggering the zero crossing detector. Consequently, selection of the X-rays is accomplished by requiring a minimum as well as a maximum acceptable rise time.

The output of the zero crossing discriminator is a fast rising and falling waveform of a nearly constant width for all X-ray energies above 2 keV. This width is converted to an amplitude in the conventional manner by means of a ramp generator. Subsequently the signal is amplified, delayed 3 μsec and stretched to a width of 1000 μsec for presentation to the telemetry transmitter.

Figure 5 shows oscilloscope photographs taken at three points in the system while a small portion of the A-CH_4 detector is being irradiated by a 5.9 keV and a 3.0 keV source of X-rays simultaneously. These are the same points referred to in Figure 1: the pre-amp output, after delay line clipping and RC differentiation, and the output of the zero crossing discriminator. The constancy of the width of the zero crossing output pulse is indicative of the uniformity of the X-ray rise time. Also included in Figure 5 are photographs of the pre-amp and zero crossing outputs when Co^{60} replaces the X-ray sources. The rise times of those pre-amp output signals are observed to be considerably longer than in the X-ray case.

RESULTS

A typical rise time spectrum of X-ray and Co^{60} events as observed in a single counter are shown in Figure 6. The X-ray energy is 5.9 keV and the Co^{60} energy interval is 4.8-7.2 keV, but spectra for the entire energy range 3-10 keV are similar. The spectra have been obtained using a multichannel pulse height analyzer to record the rise time

TABLE I

Co^{60} Acceptance with Rise Time Limits Set at 75% X-ray Acceptance		
Energy Interval	X-ray Source	Co^{60} Acceptance
2-4 keV	Ag L series	11.2%
4.8-7.2	Fe^{55}	2.5
8-12	Au L series	2.5

spectrum plus a single channel analyzer to define the energy interval of the Co^{60} events. The following characteristics are noted: a strong X-ray peak in the lowest channels and a broad spectrum with comparatively few events of short rise time for the Co^{60}. It is apparent that if a few appropriate channels are selected to define a minimum and a maximum acceptable rise time the number of Co^{60} events can be vastly reduced while most of the X-ray events are retained. Performance at three energies is listed in Table I. Under actual flight conditions noise in the telemetry system may deteriorate the sharp resolution of the X-ray rise time spectrum and consequently degrade the overall performance. Between 3 and 10 keV the optimum channel selection proved to be only slightly dependent on energy. Although rejection was still significant in the energy interval 1-2 keV, the amplitude dependence of the zero crossing detector became a factor. A two parameter analysis of energy versus rise time would probably improve the background rejection at the low energies. This will be accomplished in the forthcoming sounding rocket experiment where both the energy and rise time information of each event will appear on the telemetry records. However, it is expected that with the present system the degree of difficulty involved in obtaining a large background rejection will increase as the energy gets lower. The lower energy signals are associated with shorter ionization trails that will result in events of shorter rise time.

Hence the rise time difference between the X-ray and background events will diminish as the energy decreases. There is no apparent reason why this method of background rejection cannot be extended to higher photon energies as long as saturation of the circuit elements is avoided.

Inasmuch as the minimum rise time was limited by the frequency response of the pre-amp, it may be that increasing its bandwidth will cause the X-ray rise times to separate even further from the background. If so, improved performance will result.

No attempt was made in the course of this investigation to determine the influence of the counter geometry or the gas composition upon the background rejection capability. However, it was observed that the X-ray rise time does depend on the nature of the proportional counter gas.

REFERENCES

1. R. Giacconi, H. Gursky, F. Paolini and B. Rossi, Phys. Rev. Letters 9, 439 (1962).

2. E. Mathieson and P. W. Sanford, Proc. Int. Symp. on Nuclear Electronics, Paris (1963), p. 65.

3. H. Gursky, P. Gorenstein and R. Giacconi, Astrophys. J. 150, L75 (1967).

4. W. F. Splichal, Jr., Nucl. Instr. and Meth. 41, 156 (1966).

5. W. J. Alston and J. E. Draper, Nucl, Instr. and Meth. 35, 155 (1965).

ACKNOWLEDGMENTS

We would like to thank Dr. W. Neal of the Radioactivity Center of the Massachusetts Institute of Technology for some very valuable suggestions during the course of this investigation. At American Science and Engineering we have had a number of illuminating discussions with Dr. E. Kellogg who first pointed out to us the possibility of reducing the cosmic background in this manner, and Dr. L. Van Speybroeck who has studied various factors influencing the rise time discrimination. Dr. Herbert Gursky is to be thanked for his interest and encouragement.

This work was supported by the Office of Space Science Applications of the National Aeronautics and Space Administration under Contract NASW-1634.

FIGURE CAPTIONS

Figure 1. Idealized waveforms at three points in the system are shown for two events of different rise times. Parts (a) and (b) are taken at the output of the pre-amplifier. Parts (c) and (d) are after clipping by a shorted delay line and RC differentiation. Parts (e) and (f) show the response of the tunnel diode zero-crossing discriminator.

Figure 2. Block diagram of the elements of the rise time discrimination system.

Figure 3. Simplified diagram of the pre-amplifier.

Figure 4. Zero Crossing discriminator.

Figure 5. On the left-hand side are shown oscilloscope photographs of the waveform produced by X-rays at three points in the rise time discrimination system: pre-amplifier output (top), after delay line clipping and RC differentiation (middle); and output of the tunnel diode discriminator. The horizontal time scale is 100 nsec/division and is the same for each. A small portion of the proportional counter's area is under irradiation by 5.9 and 3 keV X-rays. The gas mixture is 1 atm of 90% A-10% CH_4. The counter voltage is 2250 V and the diameter of the center wire is .002". Shown on the right-hand side are oscilloscope photographs of the pre-amplifier output (top) and the zero crossing discriminator when the X-ray sources are replaced by Co^{60}.

Figure 6. A multichannel analyzer plot is shown of the number-rise time spectrum of 5.9 keV X-rays and Co^{60} events producing a signal corresponding to about the same energy.

IDEALIZED WAVEFORMS AT THREE POINTS IN THE RISE TIME DISCRIMINATION SYSTEM

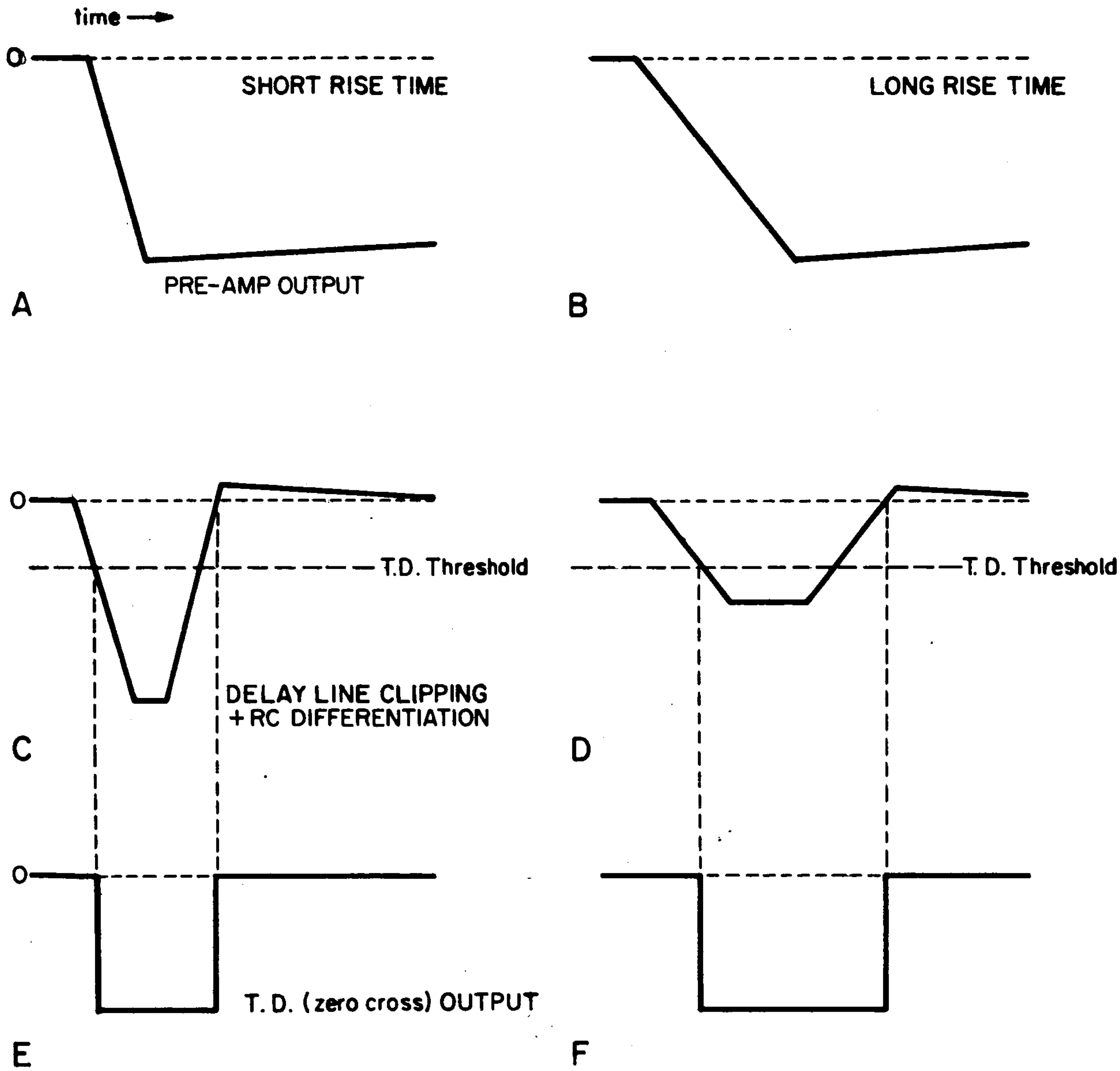

Figure 1

1825

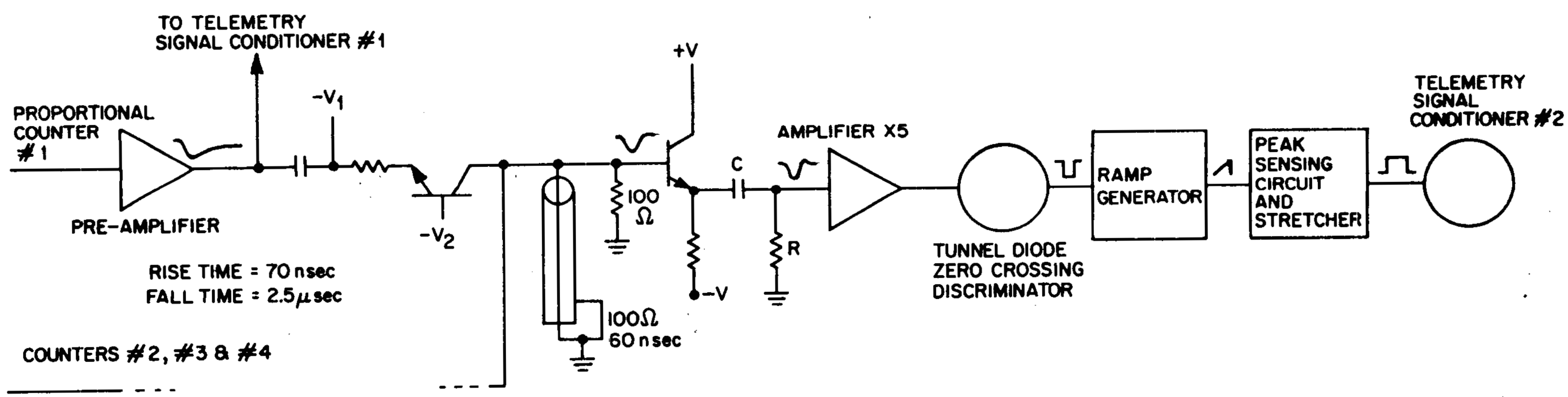

BLOCK DIAGRAM OF RISE TIME DISCRIMINATION SYSTEM

Figure 2

PROPORTIONAL COUNTER PRE-AMPLIFIER

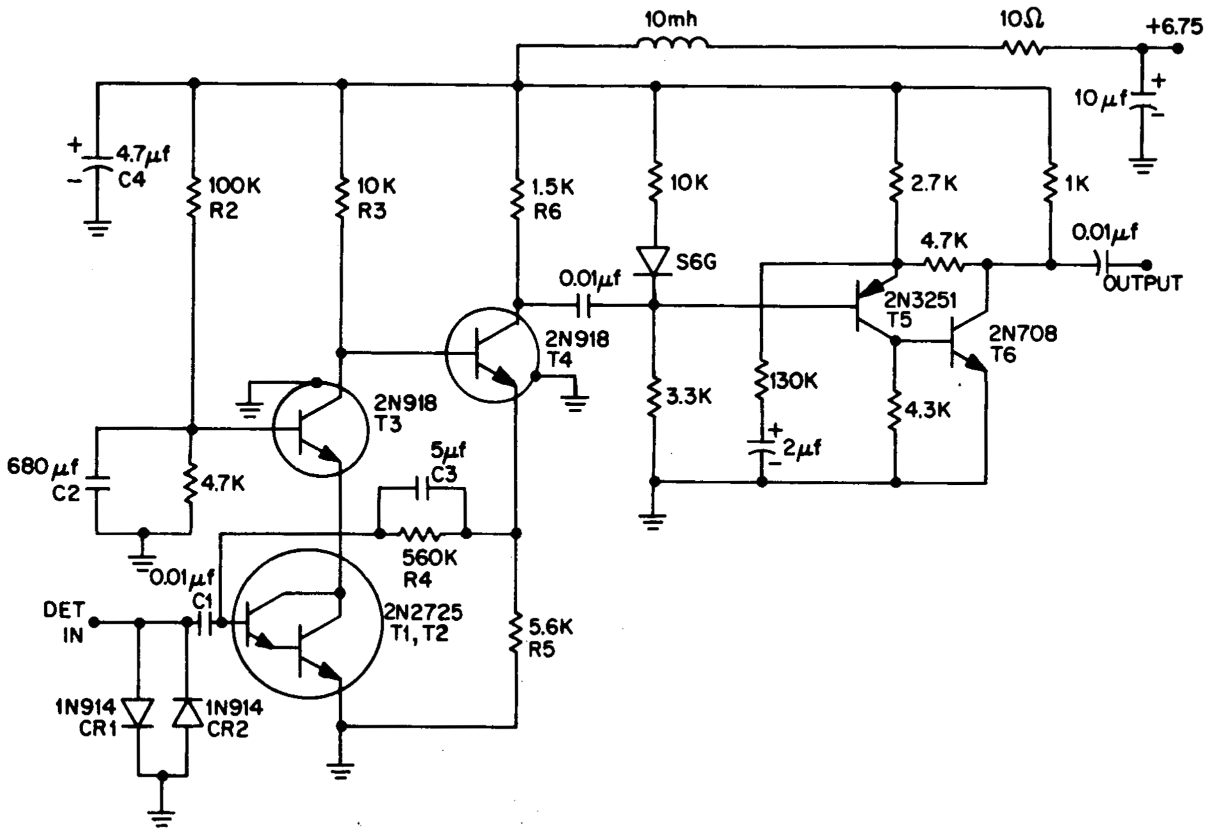

Figure 3

1825

ZERO CROSSING DISCRIMINATOR

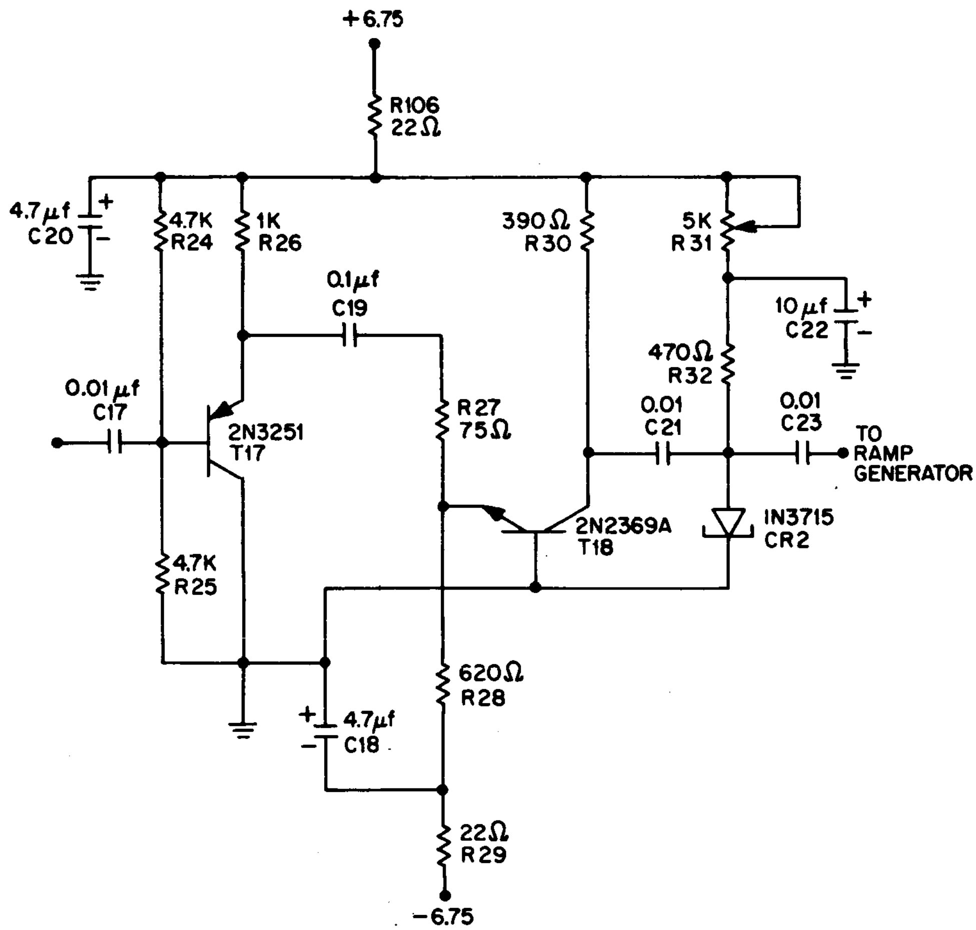

Figure 4

1825

ACTUAL WAVEFORMS FOR 3 AND 5.9 keV X-RAYS COMPARED WITH Co^{60}

HORIZONTAL SCALE .1 μSEC/DIVISION

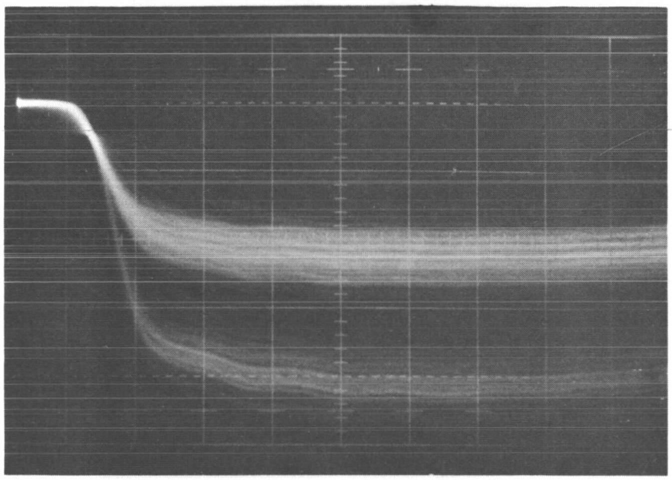

PRE-AMP OUTPUT, X-RAYS

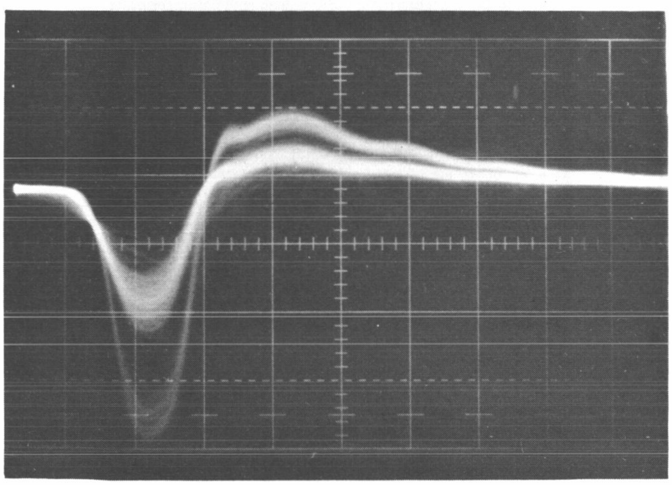

DOUBLE DIFF SIGNAL, X-RAYS

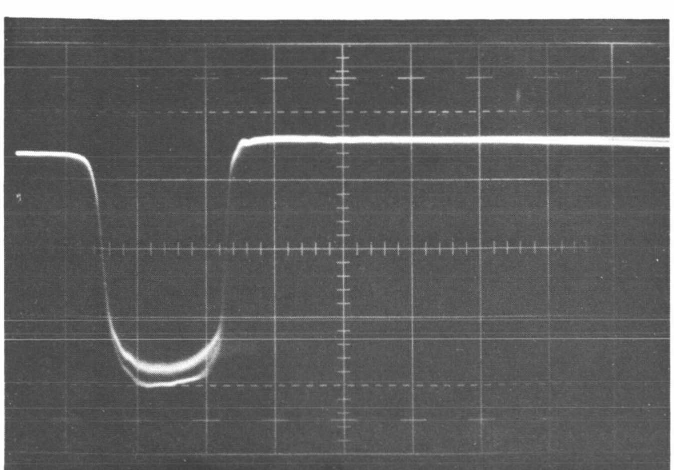

DY-006

ZERO CROSSING DISCRIMINATOR, X-RAYS

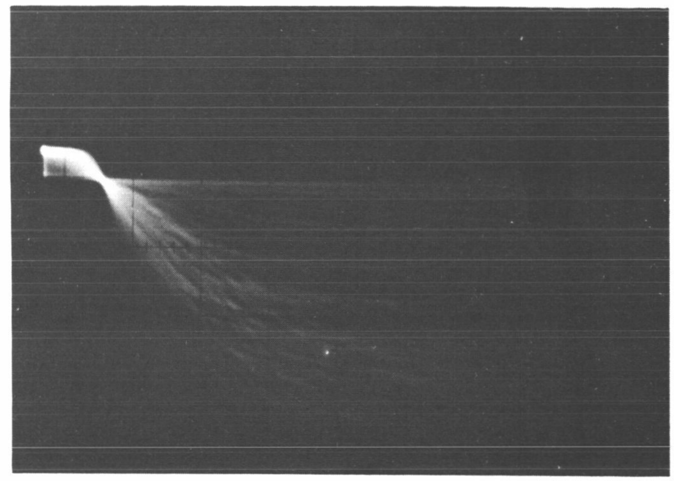

PRE-AMP OUTPUT, Co^{60}

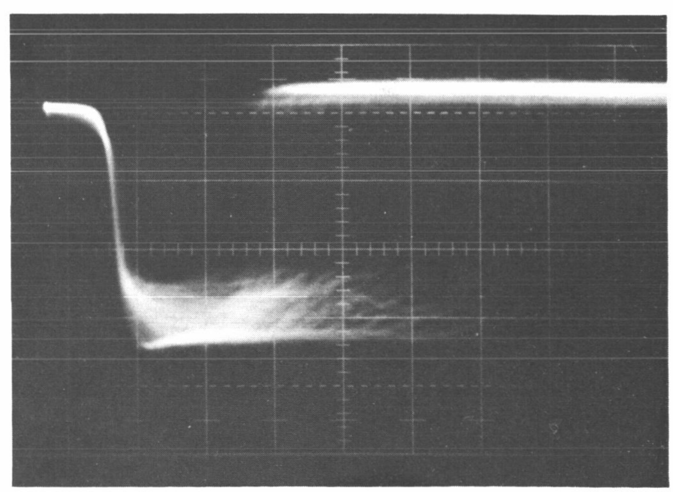

ZERO CROSSING DISCRIMINATOR, Co^{60}

Figure 5

RISE TIME SPECTRA

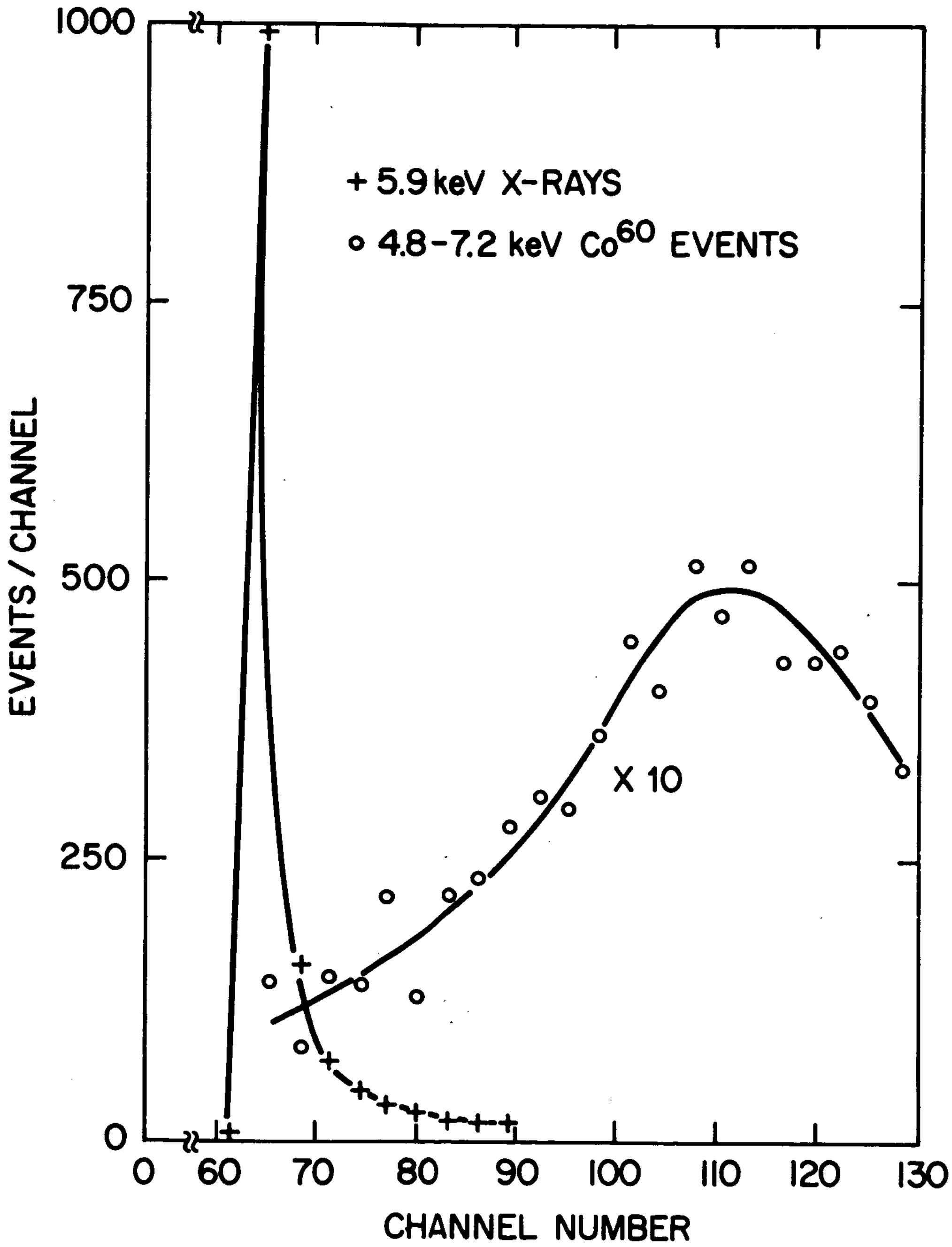

Figure 6

1825